DNA Recognition by Rhodium(III) Polyamine Intercalators: Considerations of Hydrogen Bonding and van der Waals Interactions

Achim H. Krotz, Louis Y. Kuo,† Thomas P. Shields, and Jacqueline K. Barton*

Contribution from the Division of Chemistry and Chemical Engineering, California Institute of Technology, Pasadena, California 91125

Received October 8, 1992

Abstract: A series of 9,10-phenanthrenequinone diimine (phi) complexes of rhodium have been prepared so as to systematically explore contributions of hydrogen bonding and van der Waals interactions to DNA site specificity. The novel, synthetic complexes Λ- and Δ-$[Rh(en)_2phi]^{3+}$ (**2**), as well as the analogs $[Rh(NH_3)_4phi]^{3+}$ (**1**), $[Rh([12]aneN_4)phi]^{3+}$ (**3**), and $[Rh([12]aneS_4)phi]^{3+}$ (**4**) (en = ethylenediamine, $[12]aneN_4$ = 1,4,7,10-tetraazacyclododecane, $[12]aneS_4$ = 1,4,7,10-tetrathiacyclododecane) bind in the major groove of DNA via intercalation and promote DNA strand cleavage upon activation with UV light. Complexes **1**, Δ-**2**, and **3**, all of which contain axial amines, display a high sequence preference for 5′-GC-3′ steps which is not observed for **4**. The 5′-GC-3′ preference is attributed to the hydrogen-bonding interactions between the amine ligands and the guanine O6 atoms in the major groove. Complex **4**, which lacks hydrogen bond donating groups in the axial positions, shows instead a high degree of specificity for a 5′-ATG-3′ site which is best explained by shape selection. Λ-**2** cleaves DNA with lower sequence selectivity but cleaves enantioselectively at 5′-TX-3′ steps. Photocleavage of an oligonucleotide containing the substitution of 5′-UA-3′ for 5′-TA-3′ shows no similar enantioselectivity, and hence chiral recognition of the 5′-TA-3′ step is attributed to van der Waals interactions between the methylene groups of the Λ-isomer and the thymine methyl groups in the major groove of DNA. These results provide a first example of binding and photoactivated cleavage using saturated amines and macrocyclic thioethers as ancillary ligands in DNA recognition by metallointercalators and illustrate how discrete elements of molecular recognition may direct specificity for a DNA site.

Introduction

There is substantial interest in delineating those factors which contribute to DNA site recognition by both small molecules and proteins.[1,2] Our laboratory has focused primarily upon recognition through *shape selection*.[3,4] Most recently we have explored a family of mixed ligand 9,10-phenanthrenequinone diimine (phi) polypyridyl complexes of rhodium(III).[4] Mechanistic, NMR, and DNA-binding studies have shown that these complexes associate with DNA with high affinity ($K_b \geq 10^6$ M^{-1}) in the major groove through intercalation and that the complexes display site selectivity owing to steric constraints.[4,5] Using this metallointercalation as an anchor in the major groove, we may also explore the positive contributions to site selectivity which result from noncovalent interactions, such as hydrogen bonding and van der Waals contacts. Systematic variation of the ancillary ligands in an octahedral metallointercalator allows one to probe specific contacts in the major groove.

Here we extend our studies of phi complexes of rhodium to include enantiomers of bis(ethylenediamine)(phi)rhodium(III), $[Rh(en)_2phi]^{3+}$, and their derivatives. As illustrated schematically in Figure 1, enantiomers of the novel $[Rh(en)_2phi]^{3+}$ (Λ-**2**, Δ-**2**) have been prepared, as have the analogs $[Rh(NH_3)_4phi]^{3+}$ (**1**), $[Rh([12]aneN_4)phi]^{3+}$ (**3**), and $[Rh([12]aneS_4)phi]^{3+}$ (**4**). Since these complexes are smaller than polypyridyl metallointercalators and span only one base step when intercalated into double-helical DNA, the expected level of site specificity is not high. However, these simple intercalators offer a route to examine systematically the contributions of hydrogen bonding and van der Waals contacts to site specificity, since they cleave DNA with equivalent chemistry but differ in the kind and symmetry of functional group placement with respect to the DNA groove.

Once intercalated, enantiomers of $Rh(en)_2phi^{3+}$ position coordinated axial amines for potential hydrogen bonding to the DNA helix and methylene groups for positive van der Waals contacts with the DNA bases. The enantiomers share the common placement of amines but differ in the disposition of methylene groups. The macrocyclic ligand in $[Rh([12]aneN_4)phi]^{3+}$, to a first approximation, combines the two enantiomers of $[Rh(en)_2phi]^{3+}$, while $[Rh([12]aneS_4)phi]^{3+}$ resembles the amine macrocycle but replaces amines with thioether linkages. $[Rh(NH_3)_4phi]^{3+}$ is the minimal hydrogen bonding derivative, lacking the potential for extensive van der Waals contacts and possessing only the amine hydrogen-bonding donors, as with the parent $[Rh(en)_2phi]^{3+}$. We have examined specifically how these complexes discriminate among DNA sequences through this combination of hydrogen-bonding and van der Waals interactions.

Experimental Section

Materials. 9,10-Diaminophenanthrene (DAP), ethylenediamine hydrochloride (en·2HCl), 1,4,7,10-tetraazacyclododecane ($[12]aneN_4$), and 1,4,7,10-tetrathiacyclododecane ($[12]aneS_4$) were purchased from Aldrich and were used without further purification. $RhCl_3$ was purchased from

† Present address: Department of Chemistry, Lewis and Clark College, Portland, OR 97219.

* Author to whom correspondence should be addressed.

(1) (a) Pyle, A. M.; Barton, J. K. *Prog. Inorg. Chem.* **1990**, *38*, 413. (b) Moser, H. E.; Dervan, P. B. *Science* **1987**, *238*, 645. (c) Dervan, P. B.; *Science* **1986**, *232*, 464. (d) Nicholaou, K. C.; Dai, W. M.; Tsay, S. C.; Estevez, V. A.; Wrasidlo, W. *Science* **1992**, *256*, 1172. (e) Zein, N.; Sinham; McGahren, W. J.; Ellestad, G. A. *Science* **1988**, *240*, 1198. (f) Hecht, S. M. *Acc. Chem. Res.* **1986**, *19*, 383.

(2) (a) Pabo, C. O.; Sauer, R. T. *Ann. Rev. Biochem.* **1992**, *61*, 1053. (b) Sigman, D. S. *Science* **1987**, *217*, 1197. (c) Desjarlais, J. R.; Berg, J. M. *Proc. Natl. Acad. Sci. U.S.A.* **1992**, *89*, 7345.

(3) (a) Chow, C. S.; Barton, J. K. *Methods Enzymol.* **1992**, *212*, 219. (b) Barton, J. K. *Science* **1986**, *233*, 727. (c) Kirshenbaum, M. R.; Tribolet, R.; Barton, J. K. *Nucl. Acids Res.* **1988**, *16*, 7943. (d) Mei, H. Y.; Barton, J. K. *Proc. Natl. Acad. Sci. U.S.A.* **1988**, *85*, 1339. (e) Chow, C. S.; Barton, J. K. *J. Am. Chem. Soc.* **1990**, *112*, 2839.

(4) (a) Pyle, A. M.; Long, E. C.; Barton, J. K. *J. Am. Chem. Soc.* **1989**, *111*, 4520. (b) Sitlani, A.; Long, E. C.; Pyle, A. M.; Barton, J. K. *J. Am. Chem. Soc.* **1992**, *114*, 2303. (c) Pyle, A. M.; Morii, T.; Barton, J. K. *J. Am. Chem. Soc.* **1990**, *112*, 9432–9434. (d) Chow, C. S.; Behlen, E. S.; Uhlenbeck, O. C.; Barton, J. K *Biochemistry* **1992**, *31*, 972.

(5) David, S. S.; Barton, J. K. *J. Am. Chem. Soc.* **1993**, *115*, 2984.

0002-7863/93/1515-3877$04.00/0 © 1993 American Chemical Society

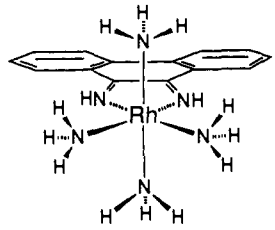

$[Rh(NH_3)_4phi]^{3+}$(1)

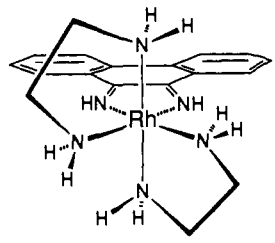

Λ-$[Rh(en)_2phi]^{3+}$(Λ-2)

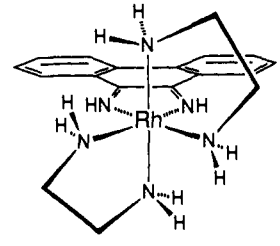

Δ-$[Rh(en)_2phi]^{3+}$(Δ-2)

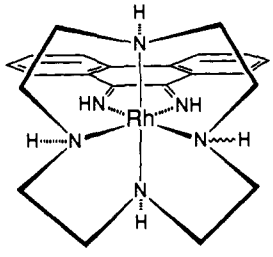

$[Rh([12]aneN_4)phi]^{3+}$(3)

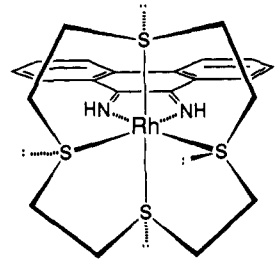

$[Rh([12]aneS_4)phi]^{3+}$(4)

Figure 1. Metallointercalators used in this study.

Aesar, Johnson-Matthey, and Aldrich. The complexes $[Rh(en)_2Cl_2]Cl$, $[Rh(NH_3)_4Cl_2]Cl$, $[Rh([12]aneN_4)Cl_2]Cl$, and $[Rh([12]aneS_4)Cl_2]Cl$ were synthesized according to published procedures.[6]

Instrumentation. Fourier-transformed ^1H NMR spectra were taken with a JEOL GX-400 spectrometer at 400 MHz or with a General Electric QE-300 spectrometer at 300 MHz in D_2O (referenced to 4.65 ppm) or DMSO-d_6 (referenced to 2.49 ppm). UV/visible spectra were recorded on a Cary 2200 spectrophotometer, and circular dichroism spectra on a JASCO J-500A spectropolarimeter. Electronic and circular dichroism spectra were recorded in a 5 mM Tris, 50 mM NaCl (pH 7.0) buffer. High-performance liquid chromatography (HPLC) was carried out using a Waters 600/600E Multi Solvent Delivery System equipped with a Waters 484 Tunable Absorbance Detector and a VYDAC Protein & Peptide C18 column. Molecular modeling was done on an Evans and Sutherland PS390 workstation using Macromodel.

Synthesis. A. Bis(ethylenediamine)(9,10-phenanthrenequinone diimine)rhodium(III) Triperchlorate, [Rh(en)$_2$phi](ClO$_4$)$_3$. Under a nitrogen atmosphere, a solution of $[Rh(en)_2Cl_2]Cl$ (600 mg, 1.9 mmol) in 4 mL of 2 N aqueous NaOH was refluxed for 30 min. After the reaction mixture was cooled to room temperature, the pH was brought to 6.2 by dropwise addition of 0.5 N $HClO_4$. Under rigorous exclusion of air, this solution was added to a degassed suspension of 9,10-diaminophenanthrene (600 mg, 2.9 mmol), $NaClO_4$ (1.6 g), and 6 mL of ethanol and was refluxed for 40 min. After the reaction mixture was cooled to room temperature, the mixture was allowed to oxidize in air overnight. The mixture was filtered, and the brownish residue was extracted several times. The filtrates were combined and purified by cation-exchange chromatography (Sephadex SP C50, eluent 0.1 N HCl then 0.5 N HCl), yield 90 mg (10%). For analytical purposes, the rhodium complex was precipitated with aqueous $NaClO_4$ solution. ^1H NMR (300 MHz, D_2O): δ (ppm) 8.17 (d, 2 H), 8.15 (d, 2 H), 7.69 (t, 2 H), 7.49 (t, 2 H), 2.55–3.10 (m, 8 H). ^{13}C NMR (75.49 MHz, D_2O): δ (ppm) 174.2, 136.4, 133.6, 129.9, 127.1, 125.0, 124.4, 45.8, 45.2. UV/vis {nm (ε[M^{-1} cm^{-1}])}: pH 7 252 (17 900), 263 (sh, 21 900), 271 (25 600), 283 (11 600), 376 (13 400), 389 (sh, 12 300). For $[Rh(en)_2phi]^{3+}$, MW = 428.9 g/mol. FAB/MS(+) (*m/z*, (assignment)): 527 (M^+ – H + ClO_4), 427 (M^+ – 2H), 463 (M^+ – H + Cl). Anal. Calc for $[Rh(en)_2phi](ClO_4)_3$, MW = 727.4: C, 29.69; H, 3.57; N, 11.54. Found: C, 29.54; H, 3.56; N, 11.16.

The crystal structure of *rac*-$[Rh(en)_2phi]Br_3 \cdot 3H_2O$ has been reported.[7]

B. Optical Resolution of [Rh(en)$_2$phi]$^{3+}$. The separation of the enantiomers of $[Rh(en)_2phi]^{3+}$ was accomplished as described by Yoshikawa and Yamasaki[8] with the following modifications. A solution of *rac*-$[Rh(en)_2phi]^{3+}$ was loaded onto a Sephadex CM-25 (40 cm × 2 cm) column. The enantiomers were resolved into two well-separated yellow bands with aqueous 0.15 M (+)-potassium antimonyl tartrate as the eluent. The first yellow band that was eluted from the column contained the (+)-antimonyl tartrate salt of the Λ-$[Rh(en)_2phi]^{3+}$ enantiomer. CD spectra of the chloride salt were recorded after ion-exchange chromatography. Δε (310 nm) = 220 deg M^{-1} cm^{-1}. Δ-$[Rh(en)_2phi]^{3+}$ displays a negative circular dichroism at 310 nm. The absolute configurations were assigned on the basis of spectral similarity to both $[Rh(en)_3]^{3+}$ and $[Rh(phen)_3]^{3+}$.[9]

C. [Rh(NH$_3$)$_4$phi]$^{3+}$ (1), [Rh([12]aneN$_4$)phi]$^{3+}$ (3), and [Rh([12]aneS$_4$)phi]$^{3+}$ (4). These complexes were made using the analogous methodology as for $[Rh(en)_2phi]^{3+}$. Full details of the synthesis, crystallography, and characterization of these novel complexes will be published separately.[10]

Methods. The 140 base pair 5′-[^{32}P]-labeled EcoRI/PvuII fragment of pUC 18 was prepared by standard methods.[11] Photoreaction conditions were 125 μM carrier DNA base pairs, 5 μM rhodium, 5 mM Tris, 50 mM NaCl, pH 7.0, irradiation at 325 nm for 30 min with a Liconix He/Cd laser. Reactions were precipitated by the addition of ethanol and dried. Pellets were suspended in loading buffer and loaded onto an 8% denaturing polyacrylamide gel. Following 3 h of electrophoresis at 1500 V, the gel was dried and placed on film. Autoradiograms were developed with a Kodak X-OMAT processor.

The oligomers L, 5′-ATATGAGCGGACATAATCGCCTGTAT-TCATAT-3′, and L-U, 5′-ATATGAGCGGACATAATCGCCTGUA-TTCATAT-3′, were synthesized on an ABI DNA synthesizer using phosphoramidite chemistry, then labeled, and isolated using established protocols.[11] The labeled oligomers were annealed with their complementary strands by heating at 90 °C for 4 min and slowly cooling to room temperature, and then incubated with metal complex, irradiated, denatured, and electrophoresed. Reaction conditions were 60 μM base pairs, 2 μM rhodium, 5 mM Tris, 50 mM NaCl, pH 7.0, irradiation at 313 nm for 30 min with an Oriel 1000-W Hg/Xe lamp, monochromator, and 305-nm cutoff filter. Following electrophoresis, the gel was wrapped in Saran Wrap and exposed to a Molecular Dynamics phosphorimager screen. Quantitation of cleavage data was made using Molecular Dynamics ImageQuant software. Cleavage at an intercalated base step was defined by the number of counts at the 5′-site in the base pair step. The extent of cleavage by a complex at the base pair step was determined first by measuring the percent counts in the site relative to the total counts in the lane including the uncut fragment, followed by subtracting the percent counts at a site for the fragment irradiated in the absence of metal complex (light control). The reproducibility in quantitation over several trials was found to be ≤3% in cleavage at an individual site.

Results and Discussion

DNA Binding and Photocleavage. The complexes resemble closely the parent $[Rh(phen)_2phi]^{3+}$ in DNA-binding and photocleavage characteristics. The complexes all display strong hypochromicity in the phi-centered $\pi \rightarrow \pi^*$ electronic transition upon titration with DNA. Hypochromicity was measured by titrating calf thymus DNA into a solution of 30 μM Rh complex to a final [DNA-base pair]/[Rh] of 10:1. The complexes Λ-**2**, **3**, and **4** display red shifts of 12, 13, and 9 nm, respectively, along

(6) (a) Dixon, N. E.; Lawrance, G. A.; Lay, P. A.; Sargeson, A. M. *Inorg. Chem.* **1984**, *23*, 2940. (b) Hancock, M. P. *Acta Chem. Scand.* **1975**, *A29*, 468. (c) Collman, J. P.; Schneider, P. W. *Inorg. Chem.* **1966**, *5*, 1380. (d) Blake, A. J.; Reid, G.; Schroder, M. *J. Chem. Soc., Dalton Trans.* **1989**, 1675.

(7) Schaefer, W. P.; Krotz, A. H.; Kuo, L. Y.; Shields, T. P.; Barton, J. K. *Acta Crystallogr.* **1992**, *C48*, 2071.

(8) Yoshikawa, Y.; Yamasaki, K. *Coord. Chem. Rev.* **1979**, *28*, 205.

(9) (a) Galbsol, F. *Inorg. Synth.* **1970**, *12*, 269. (b) Bosnich, B. *Acc. Chem. Res.* **1969**, *2*, 266.

(10) Krotz, A. H.; Shields, T. P.; Schaefer, W. P.; Barton, J. K. To be submitted.

(11) Maniatis, T.; Fritsch, E. F.; Sambrook, J. *Molecular Cloning*; Cold Spring Harbor Laboratory: 1982.

with hypochromicities of 42%, 39%, and 33%. For comparison, $[Rh(phen)_2phi]^{3+}$ displays a red shift of 16 nm and hypochromicity of 42.3% under comparable conditions.[4b] These titration experiments place a lower limit on the DNA binding affinity of 10^6 M^{-1}.

Again, like $[Rh(phen)_2phi]^{3+}$, these complexes promote the unwinding of superhelical DNA at low concentrations. The unwinding of pBR322 DNA was examined by each rhodium complex over the concentration range 1–10 μM. Comigration of form I DNA with the nicked form II was observed at 6 μM for complexes **1**, Λ-**2**, and Δ-**2**, and at 8 μM for complexes **3** and **4**.[12] For comparison, $Rh(phen)_2phi^{3+}$, which unwinds the DNA helix by 21° upon intercalation,[4b] promotes comigration of forms I and II DNA at a concentration of 6 μM rhodium by this assay.

The similarities of these new complexes to $Rh(phen)_2phi^{3+}$, with regard to unwinding of supercoiled DNA, spectroscopic changes upon DNA binding, and structure, point to common intercalative binding of all the phi complexes of rhodium with DNA. Therefore, the intercalating phi moiety may be used to direct and orient functionalities on the ancillary ligands to the DNA helix. While the unwinding and hypochromicity results alone do not locate this intercalative binding in the major groove, as has been demonstrated[4,5] for $Rh(phen)_2phi^{3+}$, the similarity in the binding characteristics of these new complexes to those of $Rh(phen)_2phi^{3+}$, as well as to those of other metallointercalators,[13,14] makes the suggestion of major-groove binding reasonable. Results described below demonstrate binding in the major groove by $[Rh(en)_2phi]^{3+}$.

Finally, these novel complexes promote DNA cleavage upon photoactivation with UV light, as does $[Rh(phen)_2phi]^{3+}$. The relative efficiency of these complexes in promoting strand cleavage using 313-nm light is of the same order of magnitude and decreases in the order $[Rh(phen)_2phi]^{3+} > [Rh([12]aneN_4)phi]^{3+} \approx [Rh(NH_3)_4phi]^{3+} \approx [Rh(en)_2phi]^{3+} > [Rh([12]aneS_4)phi]^{3+}$. Studies to correlate quantitatively the photocleavage efficiency with photoanation rate and to characterize the products of photocleavage are in progress.[15]

This study represents the first demonstration of DNA photocleavage by phi complexes of rhodium containing saturated amines and a thioether as ancillary ligands. These results indicate the generality of this photoreaction and its utility in marking sites of selective binding by novel rhodium complexes. The similarity in photocleavage characteristics also points to the similarity in binding mode and groove position for the family of complexes.

Contributions of Hydrogen Bonding to DNA Recognition. We may examine first sites which are targeted both by Δ- and Λ-$[Rh(en)_2phi]^{3+}$. Since both enantiomers share the positioning of axial amines, a similarity in cleavage sites may indicate a hydrogen-bonding contribution by the axial amines. Molecular modeling shows that, given intercalative binding, the equatorial amines are available only for hydrogen-bonding interactions with the phosphate backbone and not for base-specific interactions (vide infra). Further comparisons in cleavage to $[Rh(NH_3)_4phi]^{3+}$ and $[Rh([12]aneN_4)phi]^{3+}$, both of which contain axial amines, and to $[Rh([12]aneS_4)phi]^{3+}$, which lacks axial hydrogen-bonding functionalities, then permit the identification of the contribution of hydrogen bonding to site selectivity.

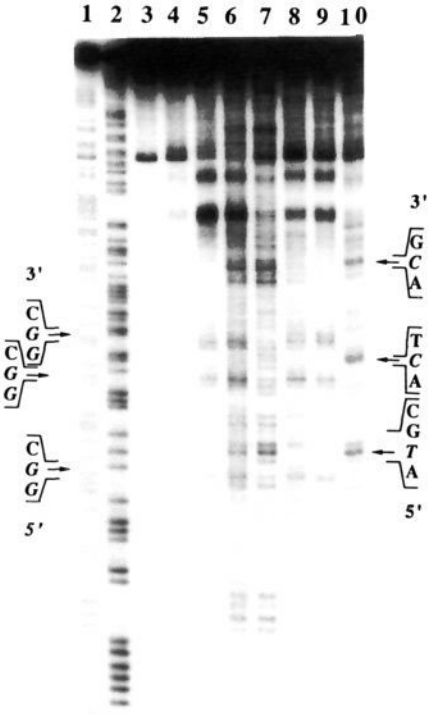

Figure 2. Recognition through hydrogen-bonding interactions. Autoradiogram of an 8% denaturing polyacrylamide gel after irradiation of a 5′-[^{32}P]-labeled EcoRI/PvuII fragment[11] of pUC 18: lanes 1 and 2, Maxam-Gilbert A+G and C+T reactions, respectively; lane 3, untreated fragment; lane 4, fragment irradiated in the absence of rhodium complex; lanes 5–10, 5′-[^{32}P]-labeled fragment irradiated in the presence of **1**, *rac*-**2**, Λ-**2**, Δ-**2**, **3**, and **4**, respectively. Some sites preferentially cleaved by the complexes containing axial amines are marked on the left with arrows. The strong cleavage sites for **4** are given on the right. Note that those complexes which contain axial hydrogen-bonding donors promote cleavage at 5′-GC-3′ sites, whereas **4**, lacking hydrogen-bonding groups, instead cleaves through shape selection at alternate sites.

Figure 2 displays an autoradiogram of an 8% denaturing polyacrylamide gel after metal-promoted DNA photocleavage on a 140 base pair restriction fragment of pUC 18. In first comparing $[Rh(en)_2phi]^{3+}$ enantiomers, overall cleavage by Λ-$[Rh(en)_2phi]^{3+}$ is seen to be higher, but there is substantial preference for Δ-$[Rh(en)_2phi]^{3+}$ cleavage at 5′-GC-3′ steps. Λ-$[Rh(en)_2phi]^{3+}$ also cleaves at these sites, but at lower intensity, since Λ-$[Rh(en)_2phi]^{3+}$ also recognizes many 5′-TX-3′ steps absent in cleavage by Δ-$[Rh(en)_2phi]^{3+}$. *rac*-$[Rh(en)_2phi]^{3+}$ shows, as expected, an additive combination of cleavage by the two enantiomers.

Photocleavage of $[Rh(en)_2phi]^{3+}$ enantiomers may be compared to that of $[Rh(NH_3)_4phi]^{3+}$, which lacks the potential for extensive van der Waals contacts and only contains hydrogen-bonding amines. Cleavage by this complex, as with Δ-$[Rh(en)_2phi]^{3+}$, is dominated by selectivity for the 5′-GC-3′ sites. Since the tetraammine complex contains only hydrogen bond donors as ancillary ligands, the high level of 5′-GC-3′ preference appears to indicate specific hydrogen bonding of the complex to guanine O6 atoms (in the major groove) above and below the intercalating base step.

Cleavage by $[Rh([12]aneN_4)phi]^{3+}$ supports this contention. This macrocyclic complex, which also contains axial amines, shows a preference for 5′-GC-3′ steps similar to that of Δ-$[Rh(en)_2phi]^{3+}$ and $[Rh(NH_3)_4phi]^{3+}$. It should be noted that $[Rh([12]aneN_4)phi]^{3+}$ appears to contain the equivalent methylenes of both

(12) Mixtures of supercoiled and nicked circular DNA were incubated with rhodium complexes and then electrophoresed through 1% agarose gels to determine the concentration of rhodium needed to achieve comigration of forms I and II. Because of the reversible dissociation of the complexes in the gel during the course of electrophoresis, these unwinding values represent substantial underestimates. No perturbations in mobility of form I DNA are observed if the metal complexes are first removed by ethanol precipitation of the DNA which establishes that the interaction is reversible..

(13) (a) Friedman, A. E.; Chambron, J.-C.; Sauvage, J.-P.; Turro, N. J.; Barton, J. K. *J. Am. Chem. Soc.* **1990**, *112*, 4960. (b) Jenkins, Y.; Friedman, A. E.; Turro, N. J.; Barton, J. K. *Biochemistry* **1992**, *31*, 10809–10816. (c) Hartshorn, R. M.; Barton, J. K. *J. Am. Chem. Soc.* **1992**, *114*, 5919.

(14) Wang, A. H. J.; Nathans, J.; van der Marel, G.; van Boom, J. H.; Rich, A. *Nature* **1978**, *276*, 471.

(15) Photoproducts following DNA damage for these complexes include both free nucleic acid bases and base propenoic acids, which is consistent with abstraction of the C3′-H atom of the deoxyribose and parallels the reactivity observed with $Rh(phen)_2phi^{3+}$.[4b]

enantiomers of $[Rh(en)_2phi]^{3+}$ and hence might be expected to resemble *rac*-$[Rh(en)_2phi]^{3+}$ in terms of cleavage characteristics. However close examination of the crystal structure[10] of $[Rh([12]aneN_4)phi]^{3+}$ reveals that the constraint of the macrocyclic ligand serves to pinch the methylene groups back from the plane perpendicular to the intercalating phi. For the series of complexes **1–3**, the N_{axial}–Rh–N_{axial} amine bond angle varies as 179.3°, 176.0°, and 160°, respectively, and the macrocyclic thioether complex **4**, is pinched back to an intermediate S_{axial}–Rh–S_{axial} angle of 168°.[10]

Importantly, $[Rh([12]aneS_4)phi]^{3+}$, which lacks hydrogen-donating functionalities, shows no preference for the 5′-GC-3′ steps but instead targets the site 5′-ATG-3′, as well as 5′-ACG-3′ and 5′-ACT-3′. It is interesting that $[Rh([12]aneS_4)phi]^{3+}$ displays strong cleavage at 5′-AXY steps, while not at other sites containing 5′-XY, since molecular modeling (*vide infra*) shows that these small metallointercalators can only span a single base step in an intercalated DNA site. No model could be built where the rhodium complex contacted the 5′-A residue when intercalated between X and Y (i.e. for a hydrogen bond donation from the A-NH_2 to the axial S) without severe propeller twisting. This recognition is therefore attributed to distortion of the helix at 5′-AXY sites, with shape selective recognition by $[Rh([12]aneS_4)phi]^{3+}$. The remarkable level of specificity by this small complex which lacks strong hydrogen-bonding groups again underscores the value of *shape selection* in achieving site recognition. It is noteworthy here that recognition may be more generally determined by more than a two-base step, despite the small size of these complexes, since inspection of the cleavage results shows consistently stronger cleavage by **1–3** at 5′-GC-3′ steps which contain a G to the 5′-side.

Also noteworthy is the strong cleavage in two regions near the 3′-end of the fragment with **1**, **Δ-2**, and **3**. These reactive sites correspond to a polypurine stretch and a 5′-GGCG-3′ step near the 3′-end. Some cleavage, though weak, is, however, also evident without metal. Perhaps local structural variations in these regions promote hypersensitivity as well as particularly strong contacts with those metal complexes which are available for hydrogen bonding.

In sum, complexes **1**, **2**, and **3**, which possess hydrogen bond donors in axial positions, display cleavage at 5′-GC-3′ steps. The preference for the 5′-GC-3′ site by $[Rh(NH_3)_4phi]^{3+}$, which contains only hydrogen-bonding groups, absent with $[Rh([12]aneS_4)phi]^{3+}$, therefore demonstrates the essentiality of hydrogen bonding in chiral recognition by Δ-$[Rh(en)_2phi]^{3+}$.

Contributions of van der Waals Contacts to DNA Recognition. Cleavage by Λ-$[Rh(en)_2phi]^{3+}$ on the above restriction fragment not only was apparent at 5′-GC-3′ steps but was also observed enantioselectively at 5′-TX-3′ steps. Since the two enantiomers present similar hydrogen bond donating axial amines, hydrogen bonding cannot account for this enantioselectivity. The preference by the Λ-isomer for 5′-TX-3′ steps suggests the possibility of van der Waals contacts between the methylene groups of the ancillary ethylenediamine ligand and the thymine methyl group, located in the major groove. The disposition of methylene groups for the Λ-isomer permits such contact; the Δ-isomer does not. No analogous interactions would be expected for the Δ-isomer at 5′-AX-3′ steps, however, given the right-handed helicity by B-DNA.

To demonstrate the involvement of specific methyl–methylene interactions in enantioselective photocleavage by the Λ-isomer at a 5′-TA-3′ step, two oligomers which contain all possible two-base steps but which differ in the substitution on both strands of U for T in a 5′-TA-3′ step were constructed, and photocleavage was examined. Enantioselectivity favoring the Λ-$[Rh(en)_2phi]^{3+}$ was observed at all 5′-TX-3′ base steps in both oligomers. These results are illustrated using a phosphorimager picture in Figure 3 and are quantitated in Table I. Importantly, removal of the methyl group in the major groove served to eliminate enantioselective cleavage. While Λ enantioselectivity is clearly evident in cleavage at the 5′-TA-3′ step, it is not observed at the 5′-UA-3′

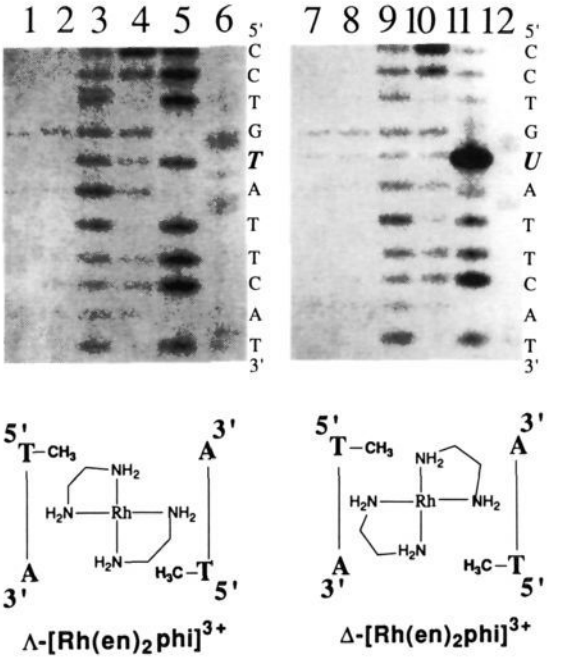

Figure 3. Recognition through specific van der Waals interactions. A (top). A segment from a phosphorimaged screen of a 20% denaturing polyacrylamide gel after irradiation of two 3′-[^{32}P]-labeled duplex oligodeoxynucleotides which differ in substitution on both strands from a 5′-TA-3′ step to a 5′-UA-3′ step. Lanes 1–6 display cleavage of the 3′-labeled L-oligomer, and lanes 7–12, cleavage of the 3′-end-labeled L-U oligomer: lanes 1 and 7, untreated oligomer; lanes 2 and 8, oligomer irradiated in absence of metal complex; lanes 3 and 9, oligomer irradiated in the presence of Λ-$[Rh(en)_2phi]^{3+}$; lanes 4 and 10, oligomer irradiated in the presence of Δ-$[Rh(en)_2phi]^{3+}$; lanes 5 and 11, Maxam–Gilbert C+T reaction; lanes 6 and 12, Maxam–Gilbert A+G reaction. These results are quantitated in Table I. Note that the photocleavage at the 5′-TA-3′ step displays a strong enantioselectivity favoring the Λ-isomer, while photocleavage at the corresponding 5′-UA-3′ step shows no enantioselectivity. B (bottom). Schematic illustrating the positioning of the methylene groups of Λ- and Δ-$[Rh(en)_2phi]^{3+}$ relative to the methyl moieties of the thymines in a 5′-TA-3′ step within an intercalation site. Note the disposition of methylenes in Λ-$[Rh(en)_2phi]^{3+}$ is poised to afford positive van der Waals interactions with the thymine methyl groups; the symmetry for the intercalated Δ-isomer does not afford similar interactions.

Table I. Enantioselectivity in Cleavage by Λ-$Rh(en)_2phi^{3+}$ at 5′-TX-3′ Steps[a,b]

base step[c]	% ee[d] at 5′-T on L	% ee[d] at 5′-T(U) on LU
5′-TA-3′ [e]	87	83
5′-TT-3′	82	78
5′-TG-3′	75	70
5′-TC-3′ [f]	34	28
5′-TA-3′ [g]	46	−4

[a] Enantioselectivities in cleavage were quantitated on the oligonucleotides L and L-U as described in the Experimental Section. [b] Less than 3% variation in cleavage intensity is observed in different trials. [c] Variations in enantioselectivities in cleavage at certain base steps have been noted as a function of nearest neighbors, and hence these results pertain only to the base pair steps on the L oligonucleotide. As a first approximation, we have defined cleavage at a base step by the cleavage intensity at the 5′-position. [d] % ee is defined as the ratio of (% cleavage by Λ − % cleavage by Δ)/(% cleavage by Λ + % cleavage by Δ) × 100. [e] Average of % ee for two 5′-(A)TA-3′ base steps. Individual values for the % ee on the L-oligomer at the two sites were 70% and 95%. [f] Average of % ee for the two 5′-TC-3′ base steps. Individual values for the % ee on the L-oligomer at the two sites were 35% and 33%. [g] This 5′-(G)TA-3′ base step was substituted with uracil on L-U.

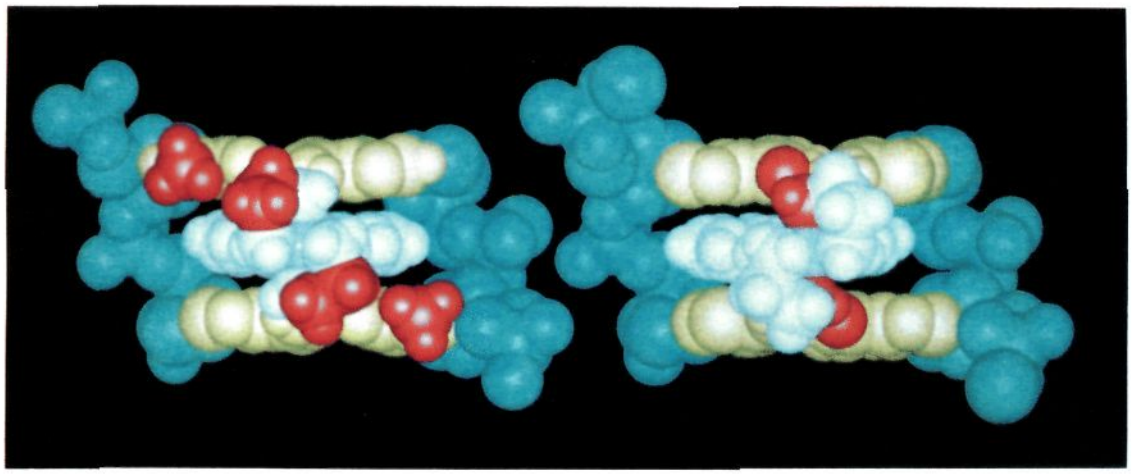

Figure 4. Molecular modeling of $[Rh(en)_2phi]^{3+}$ enantiomers in two intercalation sites. At right, Δ-$[Rh(en)_2phi]^{3+}$ is displayed intercalated into a 5′-GC-3′ step, and at left, Λ-$[Rh(en)_2phi]^{3+}$ is shown in a 5′-TA-3′ step. The interactions of interest are highlighted in red. The remainder of the metal complex is shown in white, the DNA base pairs in yellow, and the sugar–phosphate backbone in blue. The hydrogen bonding between axial amines of the complex and the 5′-guanine residues is illustrated on the right. The axial amines (in red) of Δ-$[Rh(en)_2phi]^{3+}$ are well positioned to donate a hydrogen bond to the O6 of guanine (also in red). Identical interactions are available to the axial amines of the Λ-isomer. The methylene–methyl contacts responsible for enantioselective cleavage by Λ-$[Rh(en)_2phi]^{3+}$ at 5′-TX-3′ steps are illustrated on the left. The disposition of methylene groups for Λ-$[Rh(en)_2phi]^{3+}$ complements well the positioning of the methyl groups of the thymines above and below the site of intercalation in a 5′-TA-3′ step. The methylene groups of the ethylenediamine ligands have been highlighted in red in order to show their proximity (4 Å) to the thymine methyl moieties, also in red.

step. Moreover, as apparent in Table I, little effect is seen in photocleavage at other 5′-TX-3′ steps, indicating that the local structure of the DNA is relatively unperturbed by the removal of the two methyl groups. Here recognition appears to be governed by more than the two-base step. It should be noted also that this result lends additional support to the binding of these metallointercalators in the major groove of DNA.

Most importantly, this absence of enantioselectivity at the uracil-substituted base step compared to 5′-TA-3′ demonstrates the essentiality of the thymine methyl moiety in chiral recognition by Λ-$[Rh(en)_2phi]^{3+}$. Measurements of enantioselectivity at low concentrations of rhodium on several oligonucleotides with differing nearest neighbors are in progress to quantitate this specific, noncovalent interaction with the DNA helix.

Molecular Modeling. These specific noncovalent interactions between the rigid metal complexes and the DNA helix may be illustrated using molecular modeling. Figure 4 displays models of Λ- and Δ-$[Rh(en)_2phi]^{3+}$ intercalated into 5′-TA-3′ and 5′-GC-3′ steps, respectively. The coordinates for the metal complex were taken from its crystal structure,[7] and the coordinates for the dinucleotide intercalation site in the crystal structure[14] of (terpyridyl)(ethanethiolato)platinum(II) with $d(CpG)_2$ were used for intercalative docking.[16]

As evident in Figure 4, first, the size of the metal complex is on the same order as, indeed slightly smaller than, the height along the helix axis of an intercalated base pair step. Hence at best, without conformational distortion, two-base site selectivity is expected. While two-base selectivity is apparent to a first approximation based on these results, the data also indicate an effect of nearest neighbors. The two-base site size contrasts the four-base-pair site size for the tris(phenanthroline)metal complexes and their derivatives, where the size of the complex is comparable to the size of the major groove, and overall enantioselectivities favoring the Δ-isomer are observed with right-handed DNA helices.[3b]

At the two-base level, the preferences in cleavage by Λ- and Δ-$[Rh(en)_2phi]^{3+}$ are readily illustrated with these models. As evident in Figure 4, the disposition of methylene groups for Λ-$[Rh(en)_2phi]^{3+}$ complements well the positioning of the methyl groups of thymines above and below the site of intercalation. The methylene groups of the ethylenediamine ligands have been highlighted in red in order to show their proximity to the thymine methyl moieties, also in red. The average C–C nonbonded distance is 4.0 Å in these models. In this model the distances are not too close so as to provide a steric blockade for the Λ-isomer, but sufficiently close to allow a stabilizing van der Waals contact. Clearly, a similar nonbonded contact would not be available with the Δ-isomer at the 5′-TA-3′ step. The right-handed helicity of DNA precludes a complementary interaction of the Δ-isomer at a 5′-AT-3′ step.

The appropriate positioning of the axial amines of $[Rh(en)_2phi]^{3+}$ for potential hydrogen bonding with oxygen atoms on the 5′-guanine residues is illustrated also in Figure 4. Shown in the Figure are the hydrogen-bonding interactions for Δ-$[Rh(en)_2phi]^{3+}$ with a 5′-GC-3′ base pair step, but identical hydrogen-bonding interactions would be available for the Λ-isomer. As seen in the figure, the axial amines (in red) of Δ-$[Rh(en)_2phi]^{3+}$ are well poised to donate a hydrogen bond to the O6 of guanine (also in red). N–O distances of 3.0 Å to the guanines above and below the intercalating phi may be obtained with O···H–N angles of $>160°$. It is also noteworthy that the equatorial amines are positioned only to permit hydrogen bonding to the phosphate backbone, and canting of the complex toward one strand would be required.

The interactions observed through modeling therefore bear out the results determined experimentally. The 5′-GC-3′ targeting observed with $[Rh(en)_2phi]^{3+}$, $[Rh(NH_3)_4phi]^{3+}$, and $[Rh([12]aneN_4)phi]^{3+}$ but not seen with $[Rh([12]aneS_4)phi]^{3+}$ may be attributed to specific hydrogen bonding by the axial amines of the complex. The enantioselective targeting of 5′-TX-3′ steps by Λ-$[Rh(en)_2phi]^{3+}$ is attributed to stabilizing van der Waals interactions of the methylene groups of the ethylenediamine ligands with thymine methyl groups in the DNA major groove. Once the orientation of the metal complex is determined through intercalation, the orientation of the ancillary functionalities for potential interaction with DNA becomes well defined. By delineating the hydrogen-bonding and van der Waals interactions available to these complexes and their energetic contribution,

(16) For the 5′-TA-3′ intercalation site, the structure from ref 14 was "mutated" using Macromodel.

(17) Reproducibility in quantitation of cleavage using the phosphorimager is found to be ≤3%.

one may develop a strategy for constructing transition metal complexes which bind DNA noncovalently with high sequence selectivity.

Conclusions

These results provide a first example of binding and photoactivated cleavage using saturated amines and macrocyclic thioethers as ancillary ligands in DNA recognition by metallointercalators. These metal complexes, which are wholly synthetic and can be anchored in the DNA major groove through intercalation, offer versatility in the construction of site-specific DNA-binding coordination complexes. Furthermore, the results described here illustrate how discrete elements of molecular recognition, hydrogen-bonding and van der Waals interactions, may direct specificity for a DNA site.

Acknowledgment. We are grateful to the National Institutes of Health (Grant GM33309 to J.K.B., NRSA to L.Y.K., and an NIH traineeship to T.P.S.) and the Deutsche Forschungsgemeinschaft (to A.H.K.) for their support of this research.